Dissecting Wnt/β-catenin signaling during gastrulation using RNA interference in mouse embryos

Heiko Lickert[1,*], Brian Cox[1,4], Christian Wehrle[2], Makoto M. Taketo[3], Rolf Kemler[2] and Janet Rossant[1,4,†]

[1]Samuel Lunenfeld Research Institute, Mount Sinai Hospital, Toronto M5G 1X5, Canada
[2]Max-Planck Institute of Immunobiology, Department of Molecular Embryology, Freiburg 79108, Germany
[3]Kyoto University Graduate School of Medicine, Department of Pharmacology, Yoshida-Konoe-cho, Sakyo-ku, Kyoto 606-8501, Japan
[4]University of Toronto, Department of Medical Genetics and Microbiology, Toronto M5S 1A8, Canada
*Present address: GSF – National Research Center for Environment and Health, Institute of Stem Cell Research, Neuherberg 85764, Germany
†Author for correspondence (e-mail: rossant@mshri.on.ca)

Accepted 30 March 2005

Development 132, 2599-2609
Published by The Company of Biologists 2005
doi:10.1242/dev.01842

Summary

Differential gene regulation integrated in time and space drives developmental programs during embryogenesis. To understand how the program of gastrulation is regulated by Wnt/β-catenin signaling, we have used genome-wide expression profiling of conditional β-catenin mutant embryos. Known Wnt/β-catenin target genes, known components of other signaling pathways, as well as a number of uncharacterized genes were downregulated in these mutants. To further narrow down the set of differentially expressed genes, we used whole-mount in situ screening to associate gene expression with putative domains of Wnt activity. Several potential novel target genes were identified by this means and two, *Grsf1* and *Fragilis2*, were functionally analyzed by RNA interference (RNAi) in completely embryonic stem (ES) cell-derived embryos. We show that the gene encoding the RNA-binding factor *Grsf1* is important for axial elongation, mid/hindbrain development and axial mesoderm specification, and that *Fragilis2*, encoding a transmembrane protein, regulates epithelialization of the somites and paraxial mesoderm formation. Intriguingly, the knock-down phenotypes recapitulate several aspects of Wnt pathway mutants, suggesting that these genes are components of the downstream Wnt response. This functional genomic approach allows the rapid identification of functionally important components of embryonic development from large datasets of putative targets.

Key words: Wnt/β-catenin signaling, Gastrulation, RNA interference (RNAi), Target genes, Expression profiling, *Grsf1*, *Fragilis2*, Functional genomics

Introduction

Signaling molecules of the Wnt family regulate many cellular behaviors, including differentiation, proliferation and morphogenesis, and are involved in gastrulation and axial development (reviewed by Sokol, 1999; Yamaguchi, 2001). β-Catenin, besides acting as a central component of the cadherin cell-adhesion complex, plays an essential role in the canonical Wnt/β-catenin signaling pathway (reviewed by Huber et al., 1996). Upon Wnt stimulation, β-catenin enters the nucleus and acts in a complex with members of the Tcf/Lef (T-cell factor/Lymphoid enhancer factor) family of transcription factors to activate target genes (Hecht and Kemler, 2000).

Mutations in a number of Wnt genes and Wnt signaling components highlight the crucial role of the Wnt/β-catenin signaling pathway in the initiation of primitive streak formation, as well as in the patterning and morphogenesis of the gastrulation-stage embryo (Beddington and Robertson, 1999; Lu et al., 2001). Mutant mouse embryos that lack functional Wnt3 or β-catenin fail to establish an anterior-posterior (A-P) axis and do not form a primitive streak, thus they fail to generate endoderm and mesoderm, resulting in an arrest of development before gastrulation (Liu et al., 1999; Haegel et al., 1995; Huelsken et al., 2000). Both *Wnt3a* null mutants and *Lef1;Tcf1* compound homozygous null mutants fail to differentiate paraxial mesoderm, do not form somites caudal to the forelimb buds and exhibit severe posterior truncations (Takada et al., 1994; Galceran et al., 1999). In addition, *Wnt3a* controls directly the expression of *Axin2* and *Dll1* in the paraxial mesoderm, and thereby, links the Notch and Wnt signaling pathways in the processes of somitogenesis (Aulehla et al., 2003; Galceran et al., 2004; Hofmann et al., 2004). By the end of gastrulation and the beginning of neurulation, secreted Fgf8 and Wnt1 molecules from the isthmic organizer play an important role in patterning the mid/hindbrain region along the A-P axis (reviewed by Liu and Joyner, 2001; Wurst and Bally-Cuif, 2001).

Recently, using the Cre/*loxP* system, we have conditionally inactivated β-catenin in the visceral endoderm (VE) and the anterior primitive streak (APS) by using a Cytokeration 19 (*K19*)-driven Cre (Lickert et al., 2002). Similar to in Wnt3 and β-catenin null mutants, A-P axis formation was affected; however, the conditional β-catenin mutants proceeded through gastrulation. This revealed a crucial function for β-catenin during later developmental processes, such as posterior axis

elongation and somite formation, processes affected in other Wnt mutants. Additionally, the node, an embryonic structure functionally equivalent to the Spemann/Mangold organizer in frog, failed to form in these mutants. Taken together, these results are consistent with the hypothesis that Wnt/β-catenin signaling is important for the induction of the mouse embryonic organizing centers, the formation of somites, and the proper morphogenesis of the gastrulating embryo.

Here, we have used a functional genomic approach combining Affymetrix GeneChip analysis, whole-mount in situ screening and rapid functional assessment by RNAi in embryonic stem (ES) cell-derived embryos to dissect the Wnt/β-catenin signaling pathway during gastrulation. Intriguingly, the knock-down phenotypes of two potential target genes, *Grsf1* and *Fragilis2* (*Ifitm1* – Mouse Genome Informatics), recapitulate specific but distinct aspects of Wnt pathway mutants, suggesting that these genes are components of the downstream Wnt response. In summary, this approach represents a highly efficient and rapid methodology with which to unravel developmental pathways in the mouse.

Materials and methods

Generation of mutant mice and genotyping

Cytokeratin 19 (*K19*) promoter-driven Cre mice (*K19-Cre*) were previously generated by a knock-in of the Cre recombinase gene into the ATG translation initiation codon of exon1 of *K19* (Harada et al., 1999). The β-catenin floxed (*flox*) allele and the β-catenin floxed deleted (*floxdel*) allele were previously described (Brault et al., 2001). *K19-Cre* mice were mated with β-catenin *floxdel* mice and the offspring, which inherited both alleles, were crossed with homozygous β-catenin *flox* mice; a quarter of the offspring was positive for *K19-Cre*, together with one *flox* and one *floxdel* allele. Littermates, which inherited the *floxed* and *floxdel* β-catenin alleles but did not carry the *K19-Cre* allele served as heterozygous controls. Mutant animals were bred on a mixed 129Sv×C57Bl/6 background. PCR genotyping was performed as described previously (Lickert et al., 2002).

Microarray experiments

Microarray experiments have been submitted to GEO in a MIAME compliant format (Minimum Information About a Microarray Experiment) (Brazma et al., 2001). The accession number is GSE2519.

Sample preparation

Embryos from the above described intercrosses were dissected in PBS and separated into embryonic and extraembryonic portions. The embryonic portions were stored in PBS at –80°C until the PCR genotyping was carried out using the extraembryonic portions. The pooled embryos were homogenized in 250 μl of TRIzol Reagent (Invitrogen), and total RNA was extracted according to the manufacturer's protocol.

Probe preparation and GeneChip hybridization

For each sample, 5 μg total RNA was used for cDNA synthesis according to the Expression Analysis Technical Manual (Affymetrix). The in vitro transcription and labeling of cRNA was carried out using the BioArray High-Yield Transcription Labeling Kit (Enzo). Then 25 μg of labeled cRNA was used to hybridize all three GeneChips from the Affymetrix U74v2 according to the standardized Affymetrix protocol.

Data analysis

MAS 5.0 software was used to generate the expression data set for each GeneChip.dat file and scale normalized to a target value of 150. Comparisons were made to calculate signal log ratios of expression between mut:wt and mut:het using either wild type (wt) or heterozygotes (het) as a baseline, respectively. The resulting table was exported to Microsoft Excel to filter out probe sets with absent calls across all samples (*P*-detection >0.04) and probe sets with no change in expression (0.003 > *P*-signal log ratio <0.997) in both mut:het and mut:wt comparisons. Illogical combinations of absent and present calls with a significant change call were deleted, e.g. an absent call in baseline and present call in mutant with a decrease change. Genes that were consistently up- and downregulated in both comparisons (absolute signal log ratio of ⩾0.5) were hierarchically clustered using Cluster 3.0 software [http://bonsai.ims.u-tokyo.ac.jp/~mdehoon/software/cluster/software.htm, based on the method of Eisen et al. (Eisen et al., 1998)].

Using the Affymetrix Gene Ontology (GO) analysis software (www.affymetrix.com) the numbers of probe sets on U74v2A GeneChip corresponding to the GO terms 'Transcription' (GOID:6350), 'Cell Communication' (GOID:7154), 'Pattern Specification' (GOID:7389) and 'Morphogenesis' (GOID:9653) were calculated as of the November 2003 annotation build. The total numbers of all other probe sets with a GO term were denoted as 'Others'. Additionally, the numbers for the same GO terms were calculated for the 49 downregulated genes from the U74Av2 GeneChip. Percentiles for each GO term category were calculated by dividing the numbers in each category by the total number of probe sets with any GO term.

Whole-mount in situ hybridization, histology and alkaline phosphatase staining

For whole-mount in situ hybridization and histology, embryos were processed as described previously (Lickert et al., 2002). Sense and antisense in situ probes were in vitro transcribed using ESTs available from ATCC (Manassas, VA, USA) with the following I.M.A.G.E. Clone IDs: *Fragilis2*, 657273; *Zic3*, 5120056; *Scap2*, 3599914; *Punc*, 3514346; *EST10*, 3980327; *EST16*, 1328681; *Sox2*, 5707193. Additionally, ESTs from the NIA 15K Mouse cDNA Clone Set with the following H3 clone IDs were used for probe synthesis: *Grsf1*, H3046G05; *EST6*, H3074B02. Additional probes for known genes were as follows: *Axin2* (Aulehla et al., 2003), *Wnt3a* (Gavin et al., 1990), *Wnt8* (Bouillet et al., 1996), *Frzb1* (Hoang et al., 1998), *Notch1* (Conlon et al., 1995), *Dll1* (Hrabe de Angelis et al., 1997), *Gbx2* (Wassarman et al., 1997), *Hoxb1* (Marshall et al., 1992), *T* (Herrmann et al., 1990), *Tbx6* (Chapman et al., 1996), *PAPC* (Rhee et al., 2003), and *Krox20* (Swiatek and Gridley, 1993).

To identify germ cells, embryos were fixed in 4% paraformaldehyde in PBS for 30 minutes and stained for tissue non-specific alkaline phosphatase for 5 minutes [25 mM Tris-maleic acid (pH 9.0), 0.4 mg/ml α-naphthyl phosphate (Sigma), 1 mg/ml Fast Red TR salt (Sigma), 8 mM $MgCl_2$, 0.01% Na-desoxycholate, 0.02% NP-40].

shRNA targeting of ES cells and embryos and northern blot analysis

For construction of the *Grsf1* and *Fragilis2* shRNA transgenes, we have used the pcDNA3.1 *RasGAP* shRNA plasmid described recently (Kunath et al., 2003). *RasGAP* shRNA was released from the plasmid by *Asp*718, *Xba*I digestion, and annealed oligonucleotides corresponding to the target sequence were introduced into the same sites using the following sense- and antisense-strand oligonucleotides (target sequence in bold):

Grsf1 shRNA forward, 5′-GT ACC **AAA GCA CAG GGA AGA AAT TGG TA** C AAG AGA **TA CCA ATT TCT TCC CTG TGC TTT** TTT TTGG AAA T-3′ and *Grsf1* shRNA reverse, 5′-CTA GAT TTC CAA AAA **AAA GCA CAG GGA AGA AAT TGG TA** T CTC TTG **TA CCA ATT TCT TCC CTG TGC TTT** G-3′ (corresponding

to bases 982-1004 of the murine *Grsf1* gene, NCBI accession no.: NM_178700); and

Fragilis2 shRNA forward, 5′-GT ACC **GAA CAT CAG CTC CCT GTT CTT CA** C AAG AGA **TG AAG AAC AGG GAG CTG ATG TTC** TTT TTT TGG AAA T-3′ and *Fragilis2* shRNA reverse, 5′-CTA GAT TTC CAA AAA AA **GAA CAT CAG CTC CCT GTT CTT CA** T CTC TTG **TG AAG AAC AGG GAG CTG ATG TTC** G-3′ (corresponding to bases 295-317 of the murine *Fragilis2* gene, NCBI accession no.: BK001123).

The resulting shRNA targeting constructs were confirmed by DNA sequencing. Transgenic ES-cell lines were established as described (Kunath et al., 2003). The mRNA expression level of the individual ES-cell lines for *Grsf1* and *Fragilis2* was determined by northern blotting using the NorthernMax-Gly^{TM} Kit (Ambion), according to the manufacturer's protocol. Pre-selected ES-cell lines were used to generate totally ES cell-derived embryos using the tetraploid aggregation technique as described previously (Nagy et al., 1993; Kunath et al., 2003). Embryos with any contribution of tetraploid EGFP-positive cells were excluded from the analysis. Experimental animals were treated according to guidelines approved by the Canadian Council for Animal Care.

Co-culture of ES cells with Wnt1-expressing fibroblasts

The co-cultivation of ES cells with NIH3T3 fibroblasts was carried out essentially as described previously (Lickert et al., 2000), with the exception that the ES cells were seeded in transwell filters (*Transwell*-COL, collagen-treated, 0.4 μm pore-size; Costar #3491). After 18 hours of co-cultivation, total RNA was isolated from the ES cells using the *RNeasy Mini* Kit (Qiagen). For each sample, 2 μg of RNA was treated with DNaseI and then reverse transcribed using oligo (dT)-primers and SuperSriptII reverse transcriptase (Invitrogen).

Quantitative PCR was performed using the LightCycler Fast Start DNA Master^{Plus} SYBR Green I Kit (Roche) according to the manufacturer's protocol. The following primers were used to amplify mRNAs for *Gapdh*, *Fragilis2* and *Grsf1*: *Gapdh*-fwd, 5′-ACCA-CAGTCCATGCCATCACT-3′; *Gapdh*-rev, 5′-GTCCACCACCCTG-TTGCTGTA-3′; *Fragilis2*-fwd, 5′-GGGCTCCTCG-ACCACACCTCTT-3′; *Fragilis2*-rev, 5′-CCCAGTC-GTATCACCCACCATCT-3′; *Grsf1*-fwd, GATATTCG-GCCTATGACGGCT-3′; *Grsf1*-rev, CAAAATCGA-CAGCCTCTGGAAG.

Results

Expression profiling of gastrulation stage conditional β-catenin mutants

β-Catenin homozygous null mutant embryos arrest before gastrulation (Haegel et al., 1995; Huelsken et al., 2000). To study the effects of disrupting the Wnt/β-catenin signaling pathway during gastrulation, we generated embryos that were compound heterozygous for a *floxed* β-catenin allele and a β-catenin *floxdel* allele (where exon 2-6 were removed by Cre-mediated excision), carrying the *K19-Cre* allele (hereafter termed conditional β-catenin knock out (CKO) (Lickert et al., 2002). We pooled and isolated total RNA from 47 CKO (7.32 μg), 47 heterozygous (6.12 μg), and 41 wild-type (6.44 μg) embryos between late gastrulation and head-fold stage – the time when the first phenotypic alterations can be seen. The high number of embryos collected should normalize any variation in staging. The three individual RNA samples were used for labeled cRNA preparation and GeneChip hybridizations (Affymetrix U74v2 Series containing about 36,000 probe sets). No amplification of the cRNA was used to ensure accurate representation of the individual expression profiles; however, this precludes the use of biological replicates because of limiting amounts of embryonic material. To identify genes directly or indirectly deregulated in the CKO mutant embryos, we compared wild-type (wt) and heterozygous (het) expression profiles against the mutant expression profile. For further study, we focused on the genes with consistent alterations in gene expression, i.e. those differing in both comparisons with an absolute signal log ratio ⩾0.5. This limited the set of candidates to 262 upregulated and 77 downregulated genes on the three Affymetrix GeneChips (Fig. 1A, and Table S1 in the supplementary material). Here, we concentrated only on the downregulated genes in β-catenin mutants. These genes included the previously described direct target genes *Cdx1*, brachyury (*T*), follistatin, *Axin2,* and *Dll1*, thus validating the expression profiling approach (Table 1). Downregulation of genes such as *Wnt3a*, *Tbx6*, *T*, *Notch1*,

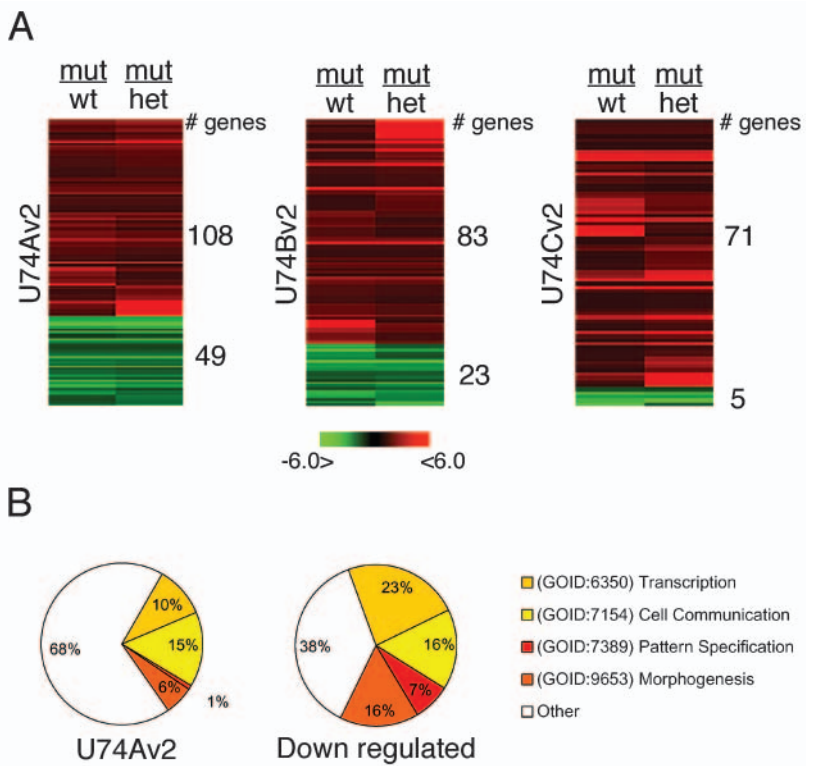

Fig. 1. Gene expression profiling of conditional β-catenin mutant embryos. (A) Hierarchical clustering of differentially regulated genes (see Materials and methods). The number of upregulated (shades of red) and downregulated (shades of green) genes per GeneChip is indicated. Different shades indicate the signal log ratios between the individual comparisons, and a color scale bar represents these values. (B) Enrichment of genes encoding for developmental regulatory factors among the potential β-catenin target genes. Approximately 6000 genes on the U74Av2 GeneChip are annotated and have a gene ontology (GOID) term. The left pie chart represents the percentage of genes with the indicated GO terms among all genes with a GO term. The right pie chart represents the percentage of genes with the indicated GO terms among the 49 downregulated genes of the U74Av2 GeneChip.

Table 1. Selected list of up- and downregulated genes

Gene symbol	Probe set ID	Mutant/wild type	Mutant/ heterozygote	GOID	Functional annotation
Sox2*	100009_r_at	1.3	1.3	(GOID:6350) Transcription	
Pem	101368_at	0.7	0.9	(GOID:6350) Transcription	
Dab2	98045_s_at	0.6	0.7	(GOID:9653) Morphogenesis	
Gbx2*	94200_at	–5.4	–4.4	(GOID:6350) Transcription	Pat
Hoxa1	95297_at	–5.1	–4.5	(GOID:7389) Pattern Specification	Pat
Cdx1	103477_at	–4.2	–4.9	(GOID:6350) Transcription	Pat
Raldh2	101707_at	–3.6	–3.4	(GOID:1523) Retinoid metabolism	Pat
twist	98028_at	–3.2	–3.6	(GOID:6350) Transcription	Pat
Hoxb1*	93888_at	–1.7	–1.8	(GOID:7389) Pattern Specification	Pat
Wnt5a	99390_at	–1.6	–1.8	(GOID:9653) Morphogenesis	Pat
Hoxb2	106927_at	–1.5	–1.4	(GOID:7389) Pattern Specification	Pat
Wnt3a*	102667_at	–2.9	–3.2	(GOID:9653) Morphogenesis	Pat, Mes
Tbx6	93611_at	–1.6	–1.8	(GOID:6350) Transcription	Pat, Mes
T	93941_at	–1.4	–1.4	(GOID:6350) Transcription	Pat, Mes
Meox1	98419_at	–1	–0.7	(GOID:6350) Transcription	Pat, Mes
FGFR1	97509_f_at	–0.6	–0.6	(GOID:7154) Cell Communication	Pat, Mes
Follistatin	98817_at	–0.6	–1	TGF-beta signaling pathway	Pat, Mes
Lef1	103628_at	–0.5	–0.6	(GOID:6350) Transcription	Pat, Mes
Axin2*	163891_at	–0.4	0.1	(GOID:7154) Cell Communication	Pat, Mes
Dll1*	92931_at	–2	–1.5	(GOID:7389) Pattern Specification	Pat, Mes, L-R
Notch1*	97497_at	–1.3	–0.8	(GOID:7389) Pattern Specification	Pat, Mes, L-R
Foxj1	98831_at	–1.2	–1	(GOID:6350) Transcription	L-R
Sox17	92996_at	–0.8	–0.7	(GOID:6350) Transcription	En
EST6†	114959_at	–5	–4.8	RIKEN cDNA C030045D06 gene	
EST16†	138065_at	–4.9	–3.7	None available	
Wnt8*	99361_at	–2.4	–3	(GOID:7154) Cell Communication	
Fragilis2†	160254_at	–1.6	–1.7	Family of IFN-inducible genes	
EST10†	97386_at	–1.5	–1.6	Similar to integrase of retrovirus	
Crabp1	98108_at	–1.5	–1.3	(GOID:5501) Retinoid binding	
Smarcd3	108488_at	–1.4	–1.5	SWI/SNF related regulator of chromatin	
NFkB	98427_s_at	–1.3	–1.1	(GOID:6350) Transcription	
Frzb1*	104672_at	–1.1	–1	(GOID:7275) Development	
Scap2†	102012_at	–1	–0.5	Src associated phosphoprotein 2	
Rbp1	104716_at	–1	–1	(GOID:1523) Retinoid metabolism	
Punc†	94117_f_at	–1	–1	(GOID:7154) Cell Communication	
Irx3	99034_at	–1	–0.9	(GOID:6350) Transcription	
AI447312	106222_at	–0.8	–1	Hypothetical aminotransferases class-II	
Grsf1†	96684_at	–0.8	–0.7	G-rich RNA sequence binding factor 1	
Zic3†	98330_at	–0.8	–0.7	(GOID:6350) Transcription	

Genes were annotated using the Affymetrix Netaffx and NCBI databases.
The Gene symbol, Affymetrix probeset ID, signal $\log_2$ ratio for both comparisons, a GO-term ID (GOID) and a functional annotation are given.
*Genes whose differential expression was confirmed by in situ hybridization.
†Genes for which the expression pattern was tested in wild-type embryos.
Pat, patterning and morphogenesis; Mes, paraxial mesoderm and somites; En, endoderm formation; L-R, left-right axis determination.

Dll1, *Meox1*, *Lef1*, follistatin, *Fgfr1* and *Axin2* is in agreement with defects in paraxial mesoderm specification and somite formation in the mutant embryos. Moreover, components of the retinoic acid signaling cascade, such as *Raldh2*, *Crabp1* and *Rbp1*, as well as components of the FGF signaling cascade, like *Fgfr1*, and components of the Wnt signaling cascade, including *Wnt3a*, *Wnt5a*, *Wnt8* and *Frzb1*, were also downregulated. These results indicate that all the major caudalizing activities were affected, offering a possible explanation for the lack of posterior development in CKO embryos. Additionally, downregulation of the general definitive endoderm marker *Sox17*, is consistent with our previous observation that endoderm formation is affected in CKO mutants. Interestingly, we also found that the downregulation of genes, like *Notch1*, *Dll1* and *Foxj1* (Krebs et al., 2003; Raya et al., 2003; Chen et al., 1998), was implicated in left-right (L-R) asymmetry (Table 1), a process not previously identified as being affected in CKO embryos and which should now be analyzed further (Lickert et al., 2002). Classification of the downregulated genes by Gene Ontology (GO) terms revealed that transcription factors, as well as genes implicated in pattern specification and morphogenesis, were highly enriched among the downregulated genes when compared with all genes on the U74Av2 GeneChip (Fig. 1B). Comparing our data with the reported expression profiles of pre-gastrulation stage β-catenin homozygous null mutants at E6.0 and E6.5 gave almost no overlap in the datasets (Morkel et al., 2003) (see Table S2 in the supplementary material), suggesting that the transcriptional Wnt response changes dynamically over the course of development.

Expression screening establishes new regulatory interactions

To confirm that downregulated genes are differentially expressed in domains of Wnt activity in wild-type and CKO embryos, in situ hybridization was performed at E7.5 (Fig. 2). Wnt ligands, such as *Wnt3a* and *Wnt8*, as well as the secreted

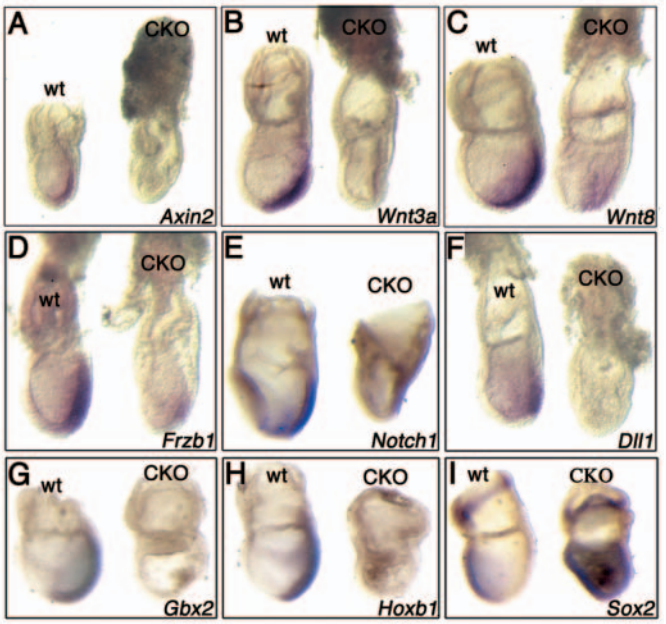

Fig. 2. Confirmation of the GeneChip results by whole-mount in situ hybridization. (A-I) Late-gastrula stage wild-type (wt) and conditional β-catenin mutant (CKO) embryos hybridized with the indicated probes. All embryos are depicted in a lateral view, anterior to the left. (A-H) *Axin2*, *Wnt3a*, *Wnt8*, *Frzb1*, *Notch1*, *Dll1*, *Gbx2* and *Hoxb1* are all expressed in the primitive streak of wild-type embryos, but are downregulated in conditional β-catenin mutants to varying extents. (I) *Sox2* is normally expressed in the extraembryonic chorion and anterior epiblast in wild-type embryos at this stage. The expression in the extraembryonic region is unaffected in mutant embryos, but the whole epiblast expresses *Sox2*.

Wnt inhibitor *Frzb1*, and the negative regulator *Axin2*, showed strong downregulation in the primitive streak (PS) of CKO embryos (Fig. 2A-D). These results suggest both positive- and negative-feedback regulation in the Wnt/β-catenin signaling pathway. We also found that the PS expression of *Notch1* and its ligand *Dll1* was downregulated in β-catenin mutants (Table 1, Fig. 2E,F). In addition, several Hox genes were downregulated in β-catenin mutants (Table 1), and *Hoxb1* was absent in β-catenin mutants (Fig. 2H). Furthermore, *Gbx2*, which is normally expressed in the posterior epiblast at late gastrulation stage (Wassarman et al., 1997), was completely lost in CKO embryos (Fig. 2G). Concordant with the loss of *Gbx2* expression, we found a posterior expansion of the expression of *Sox2*, a marker of the anterior epiblast (Fig. 2I) (Wood and Episkopou, 1999), which was upregulated in the microarray experiments (Table 1).

In summary, all nine genes tested by in situ hybridization accurately reflected the GeneChip results.

Expression screening identifies novel genes regulating embryonic development

To discover new components of Wnt/β-catenin signaling in developing embryos, we investigated further the expression of 16 downregulated genes (EST1-16) for which there was little or no published evidence concerning their developmental roles at the time the screen was conducted. Upon in situ hybridization in wild-type embryos at E7.5 and E8.5, eight of the genes showed expression patterns that strongly overlapped with known regions of high Wnt reporter activity (Fig. 3) (Mohamed et al., 2004). All genes except EST6 showed expression in the PS region at gastrulation stages (Fig. 3). In addition, *Grsf1*, *Punc* and *Zic3* showed expression in the mid/hindbrain region at E8.5, while *Scap2*, *Punc*, *Zic3*, *Fragilis2* and EST16 were expressed in the paraxial mesoderm, somites or neurectoderm of the tailbud region (Fig. 3). Interestingly, EST6 showed strong expression in the extraembryonic ectoderm and in a row of cells anterior to the node, known regions of organizing activity (Fig. 3C). EST10 showed a specific expression pattern in the definitive endoderm around gastrulation by whole-mount in situ hybridization and histological sectioning of stained embryos (Fig. 3F and data not shown).

For further analysis, we used transgenic RNA interference (RNAi) (Kunath et al., 2003) to analyze the function of the newly identified potential Wnt/β-catenin target genes, *Irx3*, *Scap2*, *Smarcd3*, *Fragilis2* and *Grsf1* (Table 1). Because the results for the *Smarcd3* knock-down analysis was recently published (Lickert et al., 2004) and because in a first attempt we were not able to knock down *Scap2* and *Irx3*, we focus here on the analysis of *Grsf1* and *Fragilis2* (Fig. 3A,G).

Knock down of potential Wnt/β-catenin targets, *Grsf1* and *Fragilis2*

Grsf1 codes for the mouse ortholog of the human G-rich sequence specific binding factor1 (GRSF1), which was previously shown to bind to a specific consensus sequence in the 5′-UTR of influenza virus nucleocapsid mRNA and thereby act positively on translation (Park et al., 1999; Kash et al., 2002). *Fragilis2* belongs to a family of interferon-inducible genes with five members (*Fragilis1-5*), clustered on 68 kb of mouse chromosome 7 and associated with germ-cell differentiation (Tanaka and Matsui, 2002; Lange et al., 2003).

Both *Grsf1* and *Fragilis2* contain several putative Wnt-responsive elements in inter- and intragenic regions (see Fig. S1 in supplementary material). To test the hypothesis that *Grsf1* and *Fragilis2* are components of the Wnt-signaling response, we first monitored mRNA expression in ES cells that had been co-cultured in transwell filters on top of Wnt1-expressing 3T3 fibroblasts (Fig. 4A) (Lickert et al., 2000). Quantitative RT-PCR revealed that Wnt1 induced endogenous *Grsf1* mRNA expression in ES cells by twofold, but had no effect on *Fragilis2* expression, which is already highly expressed in ES cells per se (Fig. 4D). We then used in situ hybridization analysis to test the mRNA expression level of both genes in wild-type and CKO embryos at E7.5 (Fig. 4B,C). Consistent with the GeneChip experiments, the expression of both genes is absent in the PS of CKO embryos, but weak *Fragilis2* expression remained at the base of the allantois, where the primordial germ cells (PGCs) are located. Because PGCs and ES cells share many molecular markers and cellular properties, this might suggest that the regulation of *Fragilis2* expression in PGCs and ES cells is independent of Wnt/β-catenin, but is dependent on this signaling system in the paraxial mesoderm emerging from the PS. This idea is further supported by transgenic enhancer studies of a PGC-specific enhancer located in intron1 of *Fragilis2*, which does not depend on two Wnt-responsive elements (data not shown).

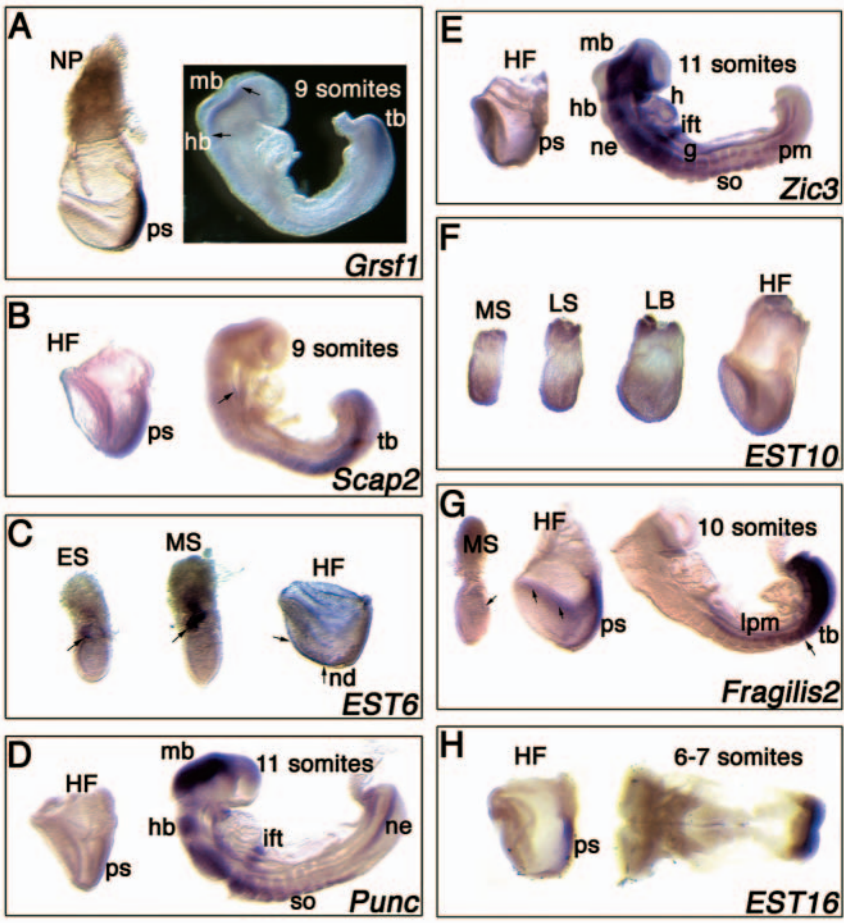

Fig. 3. Whole-mount expression screening to identify potential β-catenin target genes. (A-H) Whole-mount in situ hybridization with the indicated probes on wild-type embryos at different developmental stages. All embryos are depicted in a lateral view, anterior to the left, except for the 6- to 7-somite stage embryo in H, which is depicted in a ventral view. (A) *Grsf1* is strongly expressed in the primitive streak (ps) at neural-plate stage (NP). At 9-somite stage, *Grsf1* is restricted to the posterior neurectoderm in the tailbud (tb), and the midbrain (mb; arrow) and hindbrain region (hb; arrow). (B) *Scap2* is expressed in the primitive streak at head-fold stage. At the 9-somite stage, mRNA expression is detected in the tailbud region and foregut pocket (arrow). (C) *EST6* is expressed (arrows) in the extraembryonic ectoderm at early-streak (ES) and mid-streak (MS) stage. At head-fold stage, *EST6* shows expression in a row of cells anterior to the node (arrows). (D) *Punc* is expressed in the primitive streak at head-fold stage. At the 11-somite stage, expression is seen in the midbrain (mb) and hindbrain (hb), as well as in the somites (so), inflow tract (ift) and posterior neurectoderm. (E) *Zic3* is expressed in the primitive streak at head-fold stage. At 11-somite stage, expression is detected in anterior neurectoderm (ne), heart (h), inflow tract, gut (g), somites, midbrain (mb) and hindbrain (hb), and posterior paraxial mesoderm (pm). (F) *EST10* is strongly expressed throughout the definitive endoderm at mid-streak, late-streak (LS), late-bud (LB) and head-fold stage. (G) *Fragilis2* is first detected in the region where the allantois will form at mid-streak stage (arrow). At head-fold stage, expression is prominent in the primitive streak region and in the lateral-plate mesoderm (arrows). At 10-somite stage, expression is confined to the lateral-plate mesoderm (lpm), paraxial mesoderm and first forming somite (arrow) in the tailbud region. (H) EST16 shows expression in the primitive streak at late head-fold stage. At 6- to 7-somite stage, expression is confined to the posterior neurectoderm.

Taken together with the co-expression of *Grsf1* and *Fragilis2* in the regions of high Wnt activity, these results suggest that both genes represent good candidate Wnt/β-catenin target genes.

To test whether these genes have necessary functions in domains of Wnt activity in embryonic development, we used RNAi in ES cells (Kunath et al., 2003) to knock down *Grsf1* and *Fragilis2*. Stably transfected R1 ES-cell clones were selected and tested for successful silencing at the mRNA level using northern blotting (Fig. 4D). We were able to obtain ES-cell clones for both genes with very low residual levels of specific mRNA expression (Fig. 4D; *Grsf1*, clones 5 and 6; *Fragilis2*, clones 1 and 2), indicating that neither *Grsf1* nor *Fragilis2* function is essential for ES-cell growth or maintenance. To examine the effects of the expected silencing of these genes in embryos, we then used the tetraploid aggregation technique (Nagy et al., 1993) to generate completely ES cell-derived embryos of the efficiently silenced ES-cell lines (*Grsf1*, clones 5 and 6; *Fragilis2*, clones 1 and 2). In situ expression analysis at E7.5 revealed substantial silencing of *Grsf1* and *Fragilis2* mRNA levels, indicating that the silencing effect seen in ES cells is stably maintained in ES cell-derived embryos (Fig. 4E,F).

Grsf1 and *Fragilis2* knock downs recapitulate Wnt signaling phenotypes

Grsf1 shRNA-silenced ES cell-derived embryos did not show any obvious phenotype at E7.5 (clone 5, *n*=7; clone 6, *n*=5). At E9.5 (clone 5, *n*=10; clone 6, *n*=25), we consistently found two phenotypes: (1) truncation of the posterior axis with formation of a large allantois; and (2) abnormal mid/hindbrain development (Fig. 5A). The phenotypes observed were restricted to the expression domains of *Grsf1* in the posterior epiblast and in the mid/hindbrain region, suggesting that the effects seen are specific for *Grsf1* gene knock down (Fig. 3A). Shortening of the tailbud region was clearly seen at E8.5 (clone 5, *n*=6; clone 6, *n*=8), when the mid/hindbrain region still looked morphologically normal (Fig. 5B). The abnormally large allantois is most likely a secondary effect due to the truncation of the posterior axis and failure of chorio-allantoic fusion. A more detailed histological analysis of the mutants at E9.5 revealed an overgrowth of neurepithelium in the mid/hindbrain region of *Grsf1*-silenced embryos (Fig. 5C). Loss of epithelial integrity was seen in the neural tube from the level of the septum transversum in the midtrunk region of *Grsf1*-silenced embryos and extending posteriorly (Fig. 5D), which might be due to secondary effects, because the neural

tube rapidly degenerates following a failure of allantoic placental development. To avoid studying a secondary degeneration phenotype at this late stage, we analyzed the expression of marker genes in knock-down embryos prior to the 13-somite stage. At the 7- to 8-somite stage, *Grsf1*-silenced embryos showed slightly reduced levels of *Fgf8* expression in the isthmus region, whereas expression in the tailbud was strongly reduced (Fig. 5E) (Crossley and Martin, 1995). By the 10-somite stage, *Grsf1*-silenced embryos showed barely detectable levels of *Fgf8* in the midline of the mid/hindbrain region and almost no expression in the lateral regions of the neural tube (Fig. 5F). Expression of *Gbx2* in rhombomeres (r) 1 and 2 of knock-down embryos was strongly reduced at the 7- to 8-somite stage (Fig. 5G), whereas the hindbrain marker *Krox20* appeared to be normally expressed in r3 and r5 in these mutants (Fig. 5H). Interestingly, *Gbx2* expression in the tailbud appeared to be normal (Fig. 5G), in contrast to the reduced level of *Fgf8* in this region (Fig. 5E), which indicates that the knock down of *Grsf1* selectively alters the expression of marker genes. Onset of expression of the potential β-catenin target *Gbx2* (Fig. 2G) in the epiblast seemed to be unaffected at head-fold stage (Fig. 5I), indicating that *Grsf1* is important for maintaining *Gbx2* expression at later developmental stages in the mid/hindbrain region.

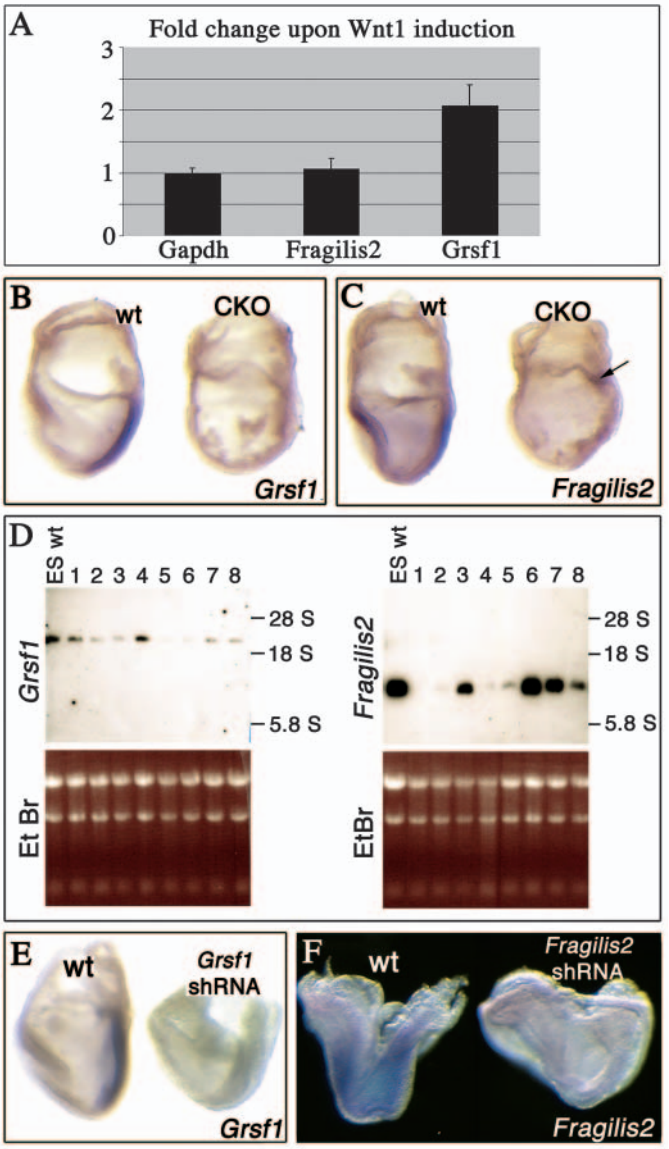

Fig. 4. The response of *Grsf1* and *Fragilis2* to Wnt signaling and shRNA silencing. (A) Co-culture of ES cells on *lacZ* and *Wnt1*-expressing fibroblasts induces *Grsf1* endogenous mRNA expression in Wnt1-treated ES cells, but not *Fragilis2* expression. Gene-specific expression was normalized to Gapdh and the fold change was calculated. Results of three independent co-culture experiments are shown. Whole-mount in situ hybridization of wild-type and β-catenin mutants (B,C), and of wild-type and shRNA-silenced embryos (E,F) with *Grsf1* and *Fragilis2* probes at late-gastrulation stage. All embryos are depicted in a lateral view, anterior to the left. *Grsf1* and *Fragilis2* are strongly downregulated in the primitive streak of β-catenin mutant embryos (B,C) and knock-down embryos (E,F). Arrow in C indicates remaining *Fragilis2* expression at the base of the allantois. (D) Northern blot analysis for *Grsf1* and *Fragilis2* for eight different shRNA ES-cell lines (1-8) and wild-type ES cells. 28S, 18S and 5.8S ribosomal RNAs are indicated as molecular length markers, and the ethidium bromide (EtBr)-stained agarose gels served as loading control.

We next tested the mRNA expression of known Wnt/β-catenin target genes, *Cdx1* and *T*, in *Grsf1* knock-down mutants. At gastrulation stages, *Cdx1* and *T* were normally expressed in the PS of mutant embryos (Fig. 5J-K), whereas the expression domain of *T* in the axial mesoderm did not extend as far anteriorly in the mutants as it did in wild-type embryos (Fig. 5K, arrows). Interestingly, *T* expression in the axial mesoderm of *Grsf1* knock-down embryos was greatly reduced at head-fold stage (Fig. 5L, arrows). Taken together, these results indicate that *Grsf1* function is essential for posterior axis elongation, midbrain development and axial mesoderm specification.

Fragilis2-silenced embryos also did not show any obvious phenotype at E7.5 (clone 1, *n*=6; clone 2, *n*=4). Embryos analyzed between E9.0 and E9.5 (clone 1, *n*=8; clone 2, *n*=13) revealed problems in somite formation and a truncation of the posterior axis (Fig. 6A). Similar to *Grsf1*-silenced embryos, *Fragilis2*-silenced embryos also developed a large allantois, presumably due to the posterior truncation. In *Fragilis2*-silenced embryos at E8.5 (clone 1, *n*=12; clone 2, *n*=8), the somites appeared hollow and were irregular in shape and smaller in size (Fig. 6B, see b′,b″). Additionally, the neural tube appeared kinked, a phenotype frequently seen in mutants affecting somite formation (Conlon et al., 1995). Histological analysis of the *Fragilis2*-silenced embryos at E8.5 revealed abnormalities in epithelialization and/or maintenance of epithelial integrity of the somites (Fig. 6C). As the Fragilis gene family is implicated in PGC development and *Fragilis2* is expressed in this cell population, we stained *Fragilis2*-silenced embryos for tissue non-specific alkaline phosphatase (AP). No difference in the AP staining between wild-type and knock-down embryos was observed, suggesting that the formation of PGCs was normal at head-fold stage (Fig. 6D).

Wnt/β-catenin signaling is implicated in both the formation of paraxial mesoderm (Takada et al., 1994; Galceran et al., 1999) and the subsequent segmentation of presomitic mesoderm into somites (Auhlela et al., 2003; Galceran et al., 2004; Hofmann et al., 2004). To discriminate between possible defects in these two processes in the *Fragilis2* knock-down embryos, we analyzed *T* and *Tbx6*, genes

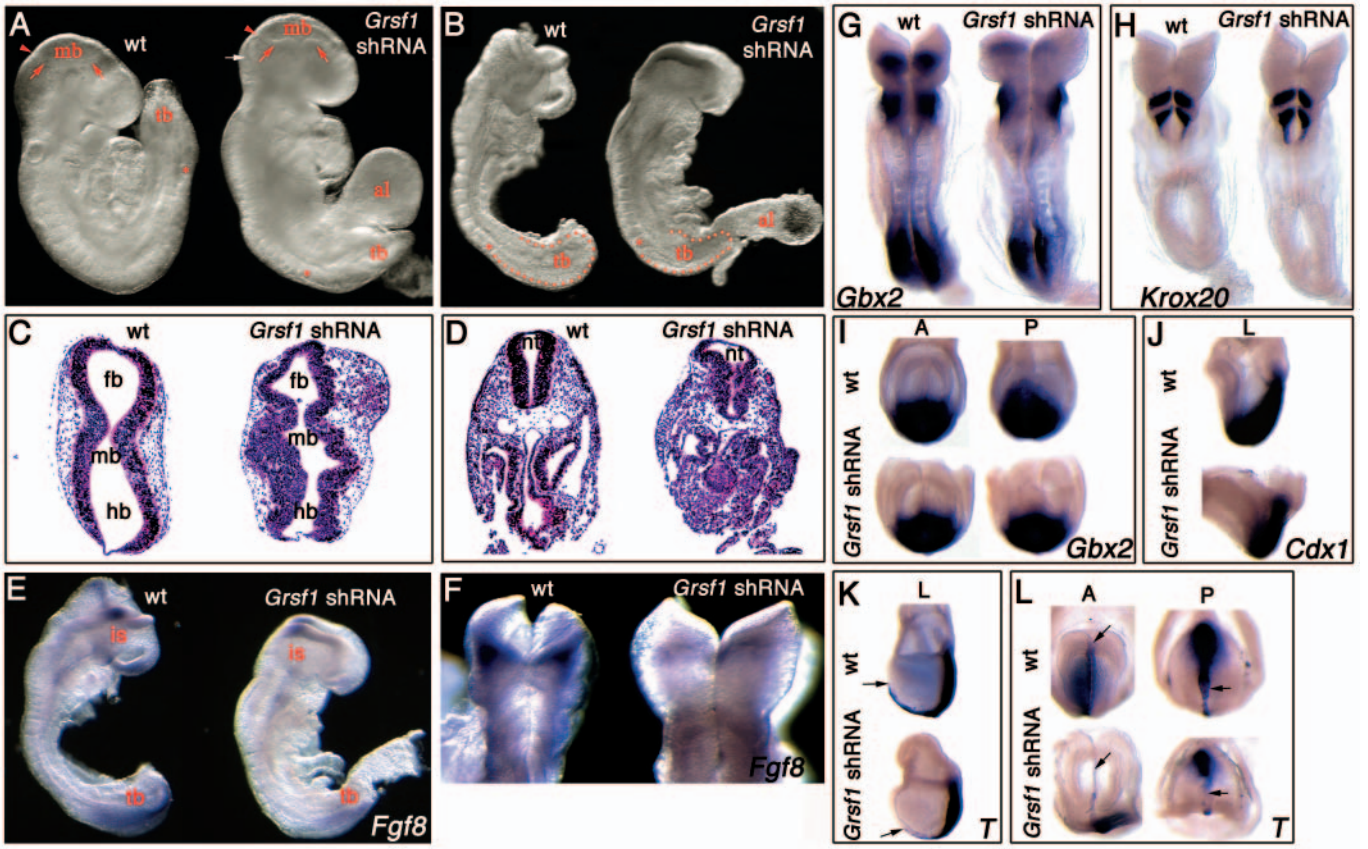

Fig. 5. *Grsf1*-silenced embryos mimic mid/hindbrain and posterior truncation phenotypes of Wnt mutants. (A) Posterior truncations are more pronounced at E9.0 (the first forming somite is indicated by an asterisk in A and B). Additionally, *Grsf1*-silenced embryos show a clear thickening in the midbrain (mb) region (red arrows), a large alantois (al) and abnormal anterior hindbrain development (white arrow; red arrowhead indicates mid/hindbrain boundary). (B) At E8.5, *Grsf1*-silenced embryos show a reduced tailbud (tb) region (indicated by dotted area). (C,D) Comparison of Hematoxylin and Eosin-stained transverse sections of wild-type and *Grsf1*-silenced embryos at E9.0. fb, forebrain; hb, hindbrain; nt, neural tube. (E-K) Whole-mount in situ analysis of wild-type and *Grsf1*-silenced embryos with indicated probes. (E,F) Comparison of *Fgf8* expression in 7-8 somite wild-type and *Grsf1*-silenced embryos. (E) Lateral view, anterior up. (F) Dorsal view on the mid/hindbrain boundary. (G,H) Comparison of hindbrain marker gene expression in wild-type and *Grsf1*-silenced embryos at 7-somite stage; dorsal view, anterior up. (I-L) Expression analysis of potential (*Gbx2*) and known Wnt/β-catenin target genes (*Cdx1* and *T*) in wt and knock-down embryos at gastrulation stage. L, lateral view, anterior to the left; A, anterior view, anterior is up; P, posterior view, posterior is up. (I,J) *Gbx2* and *Cdx1* are normally expressed in *Grsf1*-silenced embryos at head-fold stage. Note, that the posterior axis is slightly shortened in knock-down mutants. (K,L) Comparison of *T* expression in wild-type and *Grsf1*-silenced embryos at E7.5 (K) and head-fold stage (L). Arrow indicates the anterior expression border. A, anterior view; P, posterior view; L, lateral view.

implicated in paraxial mesoderm formation, and *PAPC*, a gene important for epithelialization of the somites (Rhee et al., 2003). Expression of *T* and *Tbx6* was unaffected in mutant embryos at head-fold stage, but decreased in the tailbud region at E8.5 (Fig. 5E). Expression of PAPC in wild-type embryos is restricted to two stripes at the anterior end of the presomitic mesoderm corresponding to the next two presumptive somites (Fig. 5E; somite 0 and –1). Analysis of *Fragilis2* knock-down embryos revealed that PAPC expression is decreased at head-fold stage and was barely detectable in the two presomitic stripes at 10-somite stage (Fig. 5E). Taken together, these results demonstrate that knock down of *Fragilis2* predominantly affects the epithelialization of somites, and to a lesser extent the formation of paraxial mesoderm, suggesting that *Fragilis2* acts downstream of Wnt/β-catenin to regulate these processes.

Discussion

Previous studies have highlighted the important role of Wnt/β-catenin signaling in the control of various developmental processes at the time of gastrulation and axial patterning in the early mouse embryo (Sokol, 1999; Beddington and Robertson, 1999; Yamaguchi, 2001; Lu et al., 2001). To understand mechanistically how the Wnt/β-catenin signaling cascade acts on these developmental processes, it is necessary to identify the target genes of Wnt signaling in different developmental domains. Using GeneChip analysis of conditional β-catenin mutants and wild-type embryos at late-gastrulation stages, we identified many potential Wnt/β-catenin target genes enriched for developmental components involved in pattern specification and morphogenesis, including 26 well-characterized signaling molecules and transcription factors (Table 1 and Fig. 1B). Further clustering of these genes into different functional groups, e.g. genes involved in paraxial

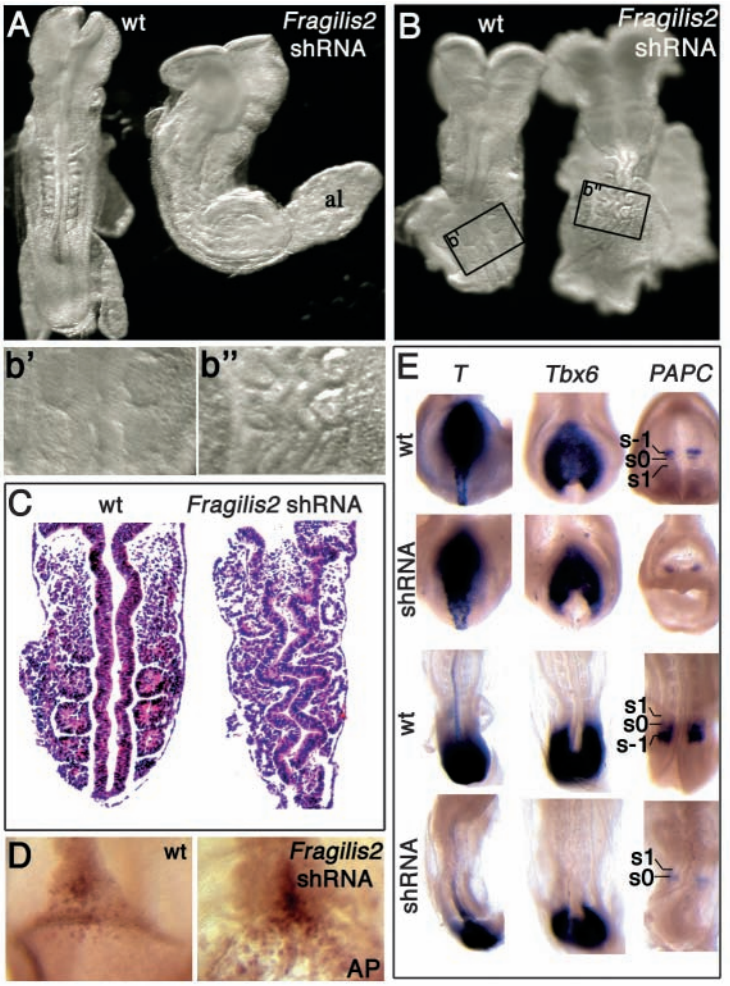

Fig. 6. *Fragilis2*-silenced embryos mimic the somite phenotype of the β-catenin mutants. (A,B,D) Embryos are depicted in a dorsal view; anterior is up. Comparison of wild-type and *Fragilis2*-silenced embryos at E8.75 (A) and E8.5 (B) demonstrates abnormal development in the posterior region, formation of a large allantois (al), a kinked neural tube and abnormal somite formation (magnified in b′ and b″). (C) Comparison of Hematoxylin and Eosin-stained frontal sections of wild-type and *Fragilis2*-silenced embryos at E8.5. (D) Tissue non-specific alkaline phosphatase (AP) staining to detect primordial germ-cell (PGC) formation at head-fold stage. Embryos are depicted in a posterior view, focusing on the embryonic-extraembryonic border. (E) Whole-mount in situ analysis of wild-type and *Fragilis2*-silenced embryos with the indicated probes at the 2- to 3-somite stage (upper panels; posterior view, posterior is up) and the 9- to 10-somite stage (lower panel; dorsal view, posterior is down). *T* and *Tbx6* are normally expressed in *Fragilis2*-silenced embryos at 2-3 somite stage, but expression is slightly reduced at the 9- to 10-somite stage in the tailbud region. In wild-type embryos, *PAPC* is expressed in two presomitic stripes (s0 and s-1). At the 2- to 3-somite stage, only one presomitic stripe is clearly visible in knock-down mutants, and *PAPC* expression further diminishes at the 9- to 10-somite stage.

mesoderm and somite formation, genes important for endoderm formation, factors involved in patterning and morphogenesis, and genes implicated in L-R axis formation (Table 1), reveals the different molecular programs potentially controlled by β-catenin during gastrulation.

As well as identifying sets of genes possibly downregulated by Wnt/β-catenin signaling at gastrulation, we also found a large number of genes that were upregulated in the conditional β-catenin mutants. One possible explanation for this is offered by the morphogenetic defects observed in β-catenin mutant embryos, such as retention of the visceral endoderm (VE) because of a lack of definitive endoderm formation, which normally displaces VE into the extraembryonic region. Consistent with this interpretation, *Dab2* and *Pem*, two marker genes for VE, were upregulated in β-catenin mutants (Table 1). However, we also found genes specifically expressed in the embryo to be upregulated, e.g. *Sox2*, an anterior epiblast marker, which later becomes restricted to the neurectoderm. In situ expression analysis showed that *Sox2* becomes expressed in the posterior region of β-catenin mutants, suggesting that the posterior epiblast has acquired an anterior fate. Further mining of the upregulated set of genes in the conditional β-catenin mutants might reveal novel components of visceral endoderm formation or anterior specification.

The objective of target gene screens is not only to identify characterized and functionally annotated genes, but also to add new players and their respective function to the gene regulatory network. All the genes we tested, whether well characterized or less well annotated, showed the expected expression differences between wild type and β-catenin mutants by in situ hybridization. Thus, we expect that our dataset will provide a rich resource for future data mining to characterize Wnt/β-catenin pathways in gastrulation. Ideally, the relative importance of target genes needs to be tested by assessing their function during development. Using shRNA-mediated gene silencing in ES cells and then in ES-derived embryos (Kunath et al., 2003), we have identified and characterized two novel putative Wnt/β-catenin target genes, *Grsf1* and *Fragilis2*, whose expression is required for normal development. Both genes, when knocked down, recapitulate specific but distinct aspects of the conditional β-catenin mutant phenotype, implicating them as crucial downstream mediators of the Wnt/β-catenin signaling pathway.

The human ortholog GRSF1 is a sequence-specific RNA-binding protein, and has been shown to act positively on translation in vitro and in a cell-culture system (Park et al., 1999; Kash et al., 2002). This raises the interesting possibility that Wnt induction of Grsf1 selectively activates the translation of other mRNA transcripts in the primitive streak and/or the mid/hindbrain region. Using a computational approach for predicting possible target genes of Grsf1, we have screened the genes expressed at late gastrulation stage according to our U74A Affymetrix wild-type data set. From 4694 annotated 5′ UTRs in the ENSEMBL database, we found 386 non-redundant genes with at least one high-affinity Grsf1 consensus binding site (5′-AGGGU-3′; see Table S3 in the supplementary material). Interestingly, among these genes we found developmental regulatory factor genes, such as *T*, *Hoxb1*, *Hoxb8* and *Frzb1,* which are co-expressed with *Grsf1* at gastrulation stage. We also found genes regulating cell proliferation, such as *p53*, cyclin B1, cyclin A2 and *Cdk2*, and genes regulating apoptosis, *Bcl2* and *Bax*, as candidate Grsf1 target genes. In-depth analysis of these potential target genes

will be required to dissect the mechanisms by which Grsf1 regulates mid/hindbrain development, posterior elongation and axial mesoderm specification.

Importantly, the observed *Grsf1* knock-down phenotypes remarkably recapitulate distinct aspects of the CKO mutant phenotype and other Wnt pathway mutants (Lickert et al., 2002; McMahon and Bradley, 1990; Thomas and Capecchi, 1990; Brault et al., 2001), suggesting that *Grsf1* is a crucial mediator of the Wnt/β-catenin signaling cascade. Interestingly, the lack of *T* expression in the anterior primitive streak of *Grsf1* knock-down embryos is comparable to lack of *T* expression in Wnt3a mutants (Yamaguchi et al., 1999), offering an explanation for the axis truncation in both mutants. The normal expression of the Wnt/β-catenin target genes, *Cdx1* and *Grsf1*, in *Grsf1* knock-down embryos suggests that Grsf1 acts downstream of the Wnt/β-catenin signaling pathway selectively on target mRNAs and is not involved in signal transduction, e.g. by stabilizing components of the pathway. This might also be the case for mid/hindbrain development, where *Grsf1* is necessary for maintaining *Fgf8* and *Gbx2* expression, two factors important for the establishment of the mid/hindbrain boundary. The comparison of putative mRNA targets of the RNA-binding factor Grsf1 (see Table S3 in the supplementary material) with all the deregulated genes from the β-catenin target gene screen (Table S1 in supplementary material) revealed several potentially co-regulated transcripts (see Table S4 supplementary material), which might explain similarities in the Grsf1 and CKO mutant phenotypes.

Fragilis2 is expressed in the primitive streak, including the base of the allantois, where the PGCs are localized at late gastrulation stage, and in the paraxial and lateral mesoderm, as well as in the first forming somites at E8.5. Studies in the immune system suggest a role for Fragilis2 (human orthologs Leu13/9-27/IFITM1) as part of a transmembrane multiprotein signaling complex implicated in inhibition of cell proliferation and homotypic cell adhesion (Knight et al., 1985; Deblandre et al., 1995; Sato et al., 1997). Histological analysis of Fragilis2-silenced embryos revealed a defect in epithelialization of the somites, consistent with a function in homotypic cell adhesion. Additionally, marker gene analysis revealed that *Fragilis2* knock-down embryos show reduced expression of PAPC, a gene implicated in somite epithelialization, and reduced expression of the paraxial mesoderm markers *T* and *Tbx6* at tailbud stage. These phenotypes are very similar to the paraxial mesoderm and somite segmentation defects seen in several different Wnt mutants (Lickert et al., 2002; Takada et al., 1994; Galceran et al., 1999; Aulehla et al., 2003; Galceran et al., 2004; Hofmann et al., 2004), thus it seems likely that *Fragilis2* is a crucial downstream mediator of the Wnt/β-catenin signaling cascade in these processes, mediating homotypic cell adhesion.

By using RNAi-mediated gene functional studies in ES cell-derived embryos, we have shown that it is possible to rapidly evaluate the relative importance of putative target genes of developmental pathways identified from expression profiling of mutant versus wild-type embryos. The potential for parallel functional analyses of several candidate genes in a relatively high throughput manner is an important component of genome-wide approaches to developmental genomics in the mouse.

We are grateful to Sue MacMaster for excellent help in the generation of chimeras. We thank Ken Harpal for help with sectioning. We thank Randy Cassada and Tilo Kunath for suggestions and critical reading of the manuscript. We are also grateful to Jerry Gish and Tony Pawson for providing us the shRNA plasmid. This work was supported by the Canadian Institutes of Health Research. H.L. was supported by a CIHR post-doctoral research fellowship and is currently supported by the Emmy-Noether fellowship from the Deutsche Forschungsgemeinschaft. J.R. is a CIHR Distinguished Scientist.

Supplementary material

Supplementary material for this article is available at
http://dev.biologists.org/cgi/content/full/132/11/2599/DC1

References

Aulehla, A., Wehrle, C., Brand-Saberi, B., Kemler, R., Gossler, A., Kanzler, B. and Herrmann, B. G. (2003). *Wnt3a* plays a major role in the segmentation clock controlling somitogenesis. *Dev. Cell* **4**, 395-406.

Beddington, R. S. and Robertson, E. J. (1999). Axis development and early asymmetry in mammals. *Cell* **96**, 195-209.

Bouillet, P., Oulad-Abdelghani, M., Ward, S. J., Bronner, S., Chambon, P. and Dolle, P. (1996). A new mouse member of the *Wnt* gene family, *mWnt-8*, is expressed during early embryogenesis and is ectopically induced by retinoic acid. *Mech. Dev.* **58**, 141-152.

Brault, V., Moore, R., Kutsch, S., Ishibashi, M., Rowitch, D. H., McMahon, A. P., Sommer, L., Boussadia, O. and Kemler, R. (2001). Inactivation of the beta-catenin gene by *Wnt1-Cre*-mediated deletion results in dramatic brain malformation and failure of craniofacial development. *Development* **128**, 1253-1264.

Brazma, A., Hingamp, P., Quackenbush, J., Sherlock, G., Spellman, P., Stoeckert, C., Aach, J., Ansorge, W., Ball, C. A., Causton, H. C. et al. (2001). Minimum information about a microarray experiment (MIAME)-toward standards for microarray data. *Nat. Genet* **29**, 365-371.

Chapman, D. L., Agulnik, I., Hancock, S., Silver, L. M. and Papaioannou, V. E. (1996). *Tbx6*, a mouse T-Box gene implicated in paraxial mesoderm formation at gastrulation. *Dev. Biol.* **180**, 534-542.

Chen, J., Knowles, H. J., Hebert, J. L. and Hackett, B. P. (1998). Mutation of the mouse hepatocyte nuclear factor/forkhead homologue 4 gene results in an absence of cilia and random left-right asymmetry. *J. Clin. Invest.* **102**, 1077-1082.

Conlon, R. A., Reaume, A. G. and Rossant, J. (1995). *Notch1* is required for the coordinate segmentation of somites. *Development* **121**, 1533-1545.

Crossley, P. H. and Martin, G. R. (1995). The mouse *Fgf8* gene encodes a family of polypeptides and is expressed in regions that direct outgrowth and patterning in the developing embryo. *Development* **121**, 439-451.

Deblandre, G. A., Marinx, O. P., Evans, S. S., Majjaj, S., Leo, O., Caput, D., Huez, G. A. and Wathelet, M. G. (1995). Expression cloning of an interferon-inducible 17-kDa membrane protein implicated in the control of cell growth. *J. Biol. Chem.* **270**, 23860-23866.

Eisen, M. B., Spellman, P. T., Brown, P. O. and Botstein, D. (1998). Cluster analysis and display of genome-wide expression patterns. *Proc. Natl. Acad. Sci. USA* **95**, 14863-14868.

Galceran, J., Farinas, I., Depew, M. J., Clevers, H. and Grosschedl, R. (1999). *Wnt3a-/–*like phenotype and limb deficiency in *Lef1(–/–)Tcf1(–/–)* mice. *Genes Dev.* **13**, 709-717.

Galceran, J., Sustmann, C., Hsu, S. C., Folberth, S. and Grosschedl, R. (2004). LEF1-mediated regulation of *Delta-like1* links *Wnt* and *Notch* signaling in somitogenesis. *Genes Dev.* **18**, 2718-2723.

Gavin, B. J., McMahon, J. A. and McMahon, A. P. (1990). Expression of multiple novel *Wnt-1/int-1*-related genes during fetal and adult mouse development. *Genes Dev.* **4**, 2319-2332.

Haegel, H., Larue, L., Ohsugi, M., Fedorov, L., Herrenknecht, K. and Kemler, R. (1995). Lack of beta-catenin affects mouse development at gastrulation. *Development* **121**, 3529-3537.

Harada, N., Tamai, Y., Ishikawa, T., Sauer, B., Takaku, K., Oshima, M. and Taketo, M. M. (1999). Intestinal polyposis in mice with a dominant stable mutation of the beta-catenin gene. *EMBO J.* **18**, 5931-5942.

Hecht, A. and Kemler, R. (2000). Curbing the nuclear activities of beta-catenin. Control over *Wnt* target gene expression. *EMBO Rep.* **1**, 24-28.

Herrmann, B. G., Labeit, S., Poustka, A., King, T. R. and Lehrach, H.

(1990). Cloning of the T gene required in mesoderm formation in the mouse. *Nature* **343**, 617-622.

Hoang, B. H., Thomas, J. T., Abdul-Karim, F. W., Correia, K. M., Conlon, R. A., Luyten, F. P. and Ballock, R. T. (1998). Expression pattern of two *Frizzled*-related genes, *Frzb-1* and *Sfrp-1*, during mouse embryogenesis suggests a role for modulating action of *Wnt* family members. *Dev. Dyn.* **212**, 364-372.

Hofmann, M., Schuster-Gossler, K., Watabe-Rudolph, M., Aulehla, A., Herrmann, B. G. and Gossler, A. (2004). *WNT* signaling, in synergy with T/TBX6, controls Notch signaling by regulating Dll1 expression in the presomitic mesoderm of mouse embryos. *Genes Dev.* **18**, 2712-2717.

Hrabe de Angelis, M., McIntyre, J., 2nd and Gossler, A. (1997). Maintenance of somite borders in mice requires the Delta homologue DII1. *Nature* **386**, 717-721.

Huber, O., Bierkamp, C. and Kemler, R. (1996). Cadherins and catenins in development. *Curr. Opin. Cell Biol.* **8**, 685-691.

Huelsken, J., Vogel, R., Brinkmann, V., Erdmann, B., Birchmeier, C. and Birchmeier, W. (2000). Requirement for beta-catenin in anterior-posterior axis formation in mice. *J. Cell Biol.* **148**, 567-578.

Kash, J. C., Cunningham, D. M., Smit, M. W., Park, Y., Fritz, D., Wilusz, J. and Katze, M. G. (2002). Selective translation of eukaryotic mRNAs: functional molecular analysis of GRSF-1, a positive regulator of influenza virus protein synthesis. *J. Virol.* **76**, 10417-10426.

Knight, E., Jr, Fahey, D. and Blomstrom, D. C. (1985). Interferon-beta enhances the synthesis of a 20,000-dalton membrane protein: a correlation with the cessation of cell growth. *J. Interferon Res.* **5**, 305-313.

Krebs, L. T., Iwai, N., Nonaka, S., Welsh, I. C., Lan, Y., Jiang, R., Saijoh, Y., O'Brien, T. P., Hamada, H. and Gridley, T. (2003). Notch signaling regulates left-right asymmetry determination by inducing *Nodal* expression. *Genes Dev.* **17**, 1207-1212.

Kunath, T., Gish, G., Lickert, H., Jones, N., Pawson, T. and Rossant, J. (2003). Transgenic RNA interference in ES cell-derived embryos recapitulates a genetic null phenotype. *Nat. Biotechnol.* **21**, 559-561.

Lange, U. C., Saitou, M., Western, P. S., Barton, S. C. and Surani, M. A. (2003). The fragilis interferon-inducible gene family of transmembrane proteins is associated with germ cell specification in mice. *BMC Dev. Biol.* **3**, 1.

Lickert, H., Domon, C., Huls, G., Wehrle, C., Duluc, I., Clevers, H., Meyer, B. I., Freund, J. N. and Kemler, R. (2000). Wnt/(beta)-catenin signaling regulates the expression of the homeobox gene *Cdx1* in embryonic intestine. *Development* **127**, 3805-3813.

Lickert, H., Kutsch, S., Kanzler, B., Tamai, Y., Taketo, M. M. and Kemler, R. (2002). Formation of multiple hearts in mice following deletion of beta-catenin in the embryonic endoderm. *Dev. Cell* **3**, 171-181.

Lickert, H., Takeuchi, J. K., von Both, I., Walls, J. R., McAuliffe, F., Adamson, S. L., Henkelman, R. M., Wrana, J. L., Rossant, J. and Bruneau, B. G. (2004). Baf60c is essential for function of BAF chromatin remodelling complexes in heart development. *Nature* **432**, 107-112.

Liu, A. and Joyner, A. L. (2001). Early anterior/posterior patterning of the midbrain and cerebellum. *Annu. Rev. Neurosci.* **24**, 869-896.

Liu, P., Wakamiya, M., Shea, M. J., Albrecht, U., Behringer, R. R. and Bradley, A. (1999). Requirement for *Wnt3* in vertebrate axis formation. *Nat. Genet.* **22**, 361-365.

Lu, C. C., Brennan, J. and Robertson, E. J. (2001). From fertilization to gastrulation: axis formation in the mouse embryo. *Curr. Opin. Genet. Dev.* **11**, 384-392.

Marshall, H., Nonchev, S., Sham, M. H., Muchamore, I., Lumsden, A. and Krumlauf, R. (1992). Retinoic acid alters hindbrain *Hox* code and induces transformation of rhombomeres 2/3 into a 4/5 identity. *Nature* **360**, 737-741.

McMahon, A. P. and Bradley, A. (1990). The *Wnt-1* (int-1) proto-oncogene is required for development of a large region of the mouse brain. *Cell* **62**, 1073-1085.

Mohamed, O. A., Clarke, H. J. and Dufort, D. (2004). Beta-catenin signaling marks the prospective site of primitive streak formation in the mouse embryo. *Dev. Dyn.* **231**, 416-424.

Morkel, M., Huelsken, J., Wakamiya, M., Ding, J., van de Wetering, M., Clevers, H., Taketo, M. M., Behringer, R. R., Shen, M. M. and Birchmeier, W. (2003). {beta}-Catenin regulates Cripto- and Wnt3-dependent gene expression programs in mouse axis and mesoderm formation. *Development* **130**, 6283-6294.

Nagy, A., Rossant, J., Nagy, R., Abramow-Newerly, W. and Roder, J. C. (1993). Derivation of completely cell culture-derived mice from early-passage embryonic stem cells. *Proc. Natl. Acad. Sci. USA* **90**, 8424-8428.

Park, Y. W., Wilusz, J. and Katze, M. G. (1999). Regulation of eukaryotic protein synthesis: selective influenza viral mRNA translation is mediated by the cellular RNA-binding protein GRSF-1. *Proc. Natl. Acad. Sci. USA* **96**, 6694-6699.

Raya, A., Kawakami, Y., Rodriguez-Esteban, C., Buscher, D., Koth, C. M., Itoh, T., Morita, M., Raya, R. M., Dubova, I., Bessa, J. G. et al. (2003). Notch activity induces *Nodal* expression and mediates the establishment of left-right asymmetry in vertebrate embryos. *Genes Dev.* **17**, 1213-1218.

Rhee, J., Takahashi, Y., Saga, Y., Wilson-Rawls, J. and Rawls, A. (2003). The protocadherin papc is involved in the organization of the epithelium along the segmental border during mouse somitogenesis. *Dev. Biol.* **254**, 248-261.

Sato, S., Miller, A. S., Howard, M. C. and Tedder, T. F. (1997). Regulation of B lymphocyte development and activation by the CD19/CD21/CD81/Leu 13 complex requires the cytoplasmic domain of CD19. *J. Immunol.* **159**, 3278-3287.

Schwartz, S., Zhang, Z., Frazer, K. A., Smit, A., Riemer, C., Bouck, J., Gibbs, R., Hardison, R. and Miller, W. (2000). PipMaker – a web server for aligning two genomic DNA sequences. *Genome Res.* **10**, 577-586.

Sokol, S. Y. (1999). *Wnt* signaling and dorso-ventral axis specification in vertebrates. *Curr. Opin. Genet. Dev.* **9**, 405-410.

Swiatek, P. J. and Gridley, T. (1993). Perinatal lethality and defects in hindbrain development in mice homozygous for a targeted mutation of the zinc finger gene *Krox20*. *Genes Dev.* **7**, 2071-2084.

Takada, S., Stark, K. L., Shea, M. J., Vassileva, G., McMahon, J. A. and McMahon, A. P. (1994). *Wnt-3a* regulates somite and tailbud formation in the mouse embryo. *Genes Dev.* **8**, 174-189.

Tanaka, S. S. and Matsui, Y. (2002). Developmentally regulated expression of mil-1 and mil-2, mouse interferon-induced transmembrane protein like genes, during formation and differentiation of primordial germ cells. *Gene Exp. Patterns* **2**, 297-303.

Thomas, K. R. and Capecchi, M. R. (1990). Targeted disruption of the murine int-1 proto-oncogene resulting in severe abnormalities in midbrain and cerebellar development. *Nature* **346**, 847-850.

Wassarman, K. M., Lewandoski, M., Campbell, K., Joyner, A. L., Rubenstein, J. L., Martinez, S. and Martin, G. R. (1997). Specification of the anterior hindbrain and establishment of a normal mid/hindbrain organizer is dependent on *Gbx2* gene function. *Development* **124**, 2923-2934.

Wood, H. B. and Episkopou, V. (1999). Comparative expression of the mouse *Sox1*, *Sox2* and *Sox3* genes from pre-gastrulation to early somite stages. *Mech. Dev.* **86**, 197-201.

Wurst, W. and Bally-Cuif, L. (2001). Neural plate patterning: upstream and downstream of the isthmic organizer. *Nat. Rev. Neurosci.* **2**, 99-108.

Yamaguchi, T. P. (2001). Heads or tails: *Wnts* and anterior-posterior patterning. *Curr. Biol.* **11**, R713-R724.

Yamaguchi, T. P., Takada, S., Yoshikawa, Y., Wu, N. and McMahon, A. P. (1999). T (Brachyury) is a direct target of *Wnt3a* during paraxial mesoderm specification. *Genes Dev.* **13**, 3185-3190.